Functional Nanofibers

DOI: 10.1002/ange.200801496

Lateral Association of Cylindrical Nanofibers into Flat Ribbons Triggered by "Molecular Glue"**

*Eunji Lee, Jung-Keun Kim, and Myongsoo Lee**

The development of novel functional materials based on self-associating block molecules has received a great deal of attention because of their potential for the construction of elaborately defined supramolecular nanostructures.[1] For example, the incorporation of a rigid aromatic segment into amphiphilic molecular architectures enhances their capability to form aggregates, leading to the assembly of a variety of nanostructures including spheres, toroids, ribbons, and tubes, depending on the structure of the component molecules.[2,3] Among the nanostructures formed by the self-assembly of specifically designed molecules, a 1D fibrillar assembly has proved to be particularly interesting for applications such as nanowires, gels, and biomemetic systems.[4] The scope of 1D structures with stimulus-responsive properties is likely to be further extended towards the area of smart nanoscale materials. We have shown that the conformational change that coordination polymers undergo upon counteranion exchange gives rise to a significant structural change from elongated fibers into discrete aggregates, which results in sol–gel interconversion.[5a] We have also shown that T-shaped aromatic amphiphiles based on oligoether dendrons self-assemble into thermoresponsive nanofibers by the reversible dehydration of external oligoether chains.[5b]

We have recently demonstrated that structural inversion of the cylindrical core formed by the self-assembly of wedge-coil block molecules based on a hydrophobic branched segment led to a reversible switching between rigid rodlike and flexible coil-like aggregates that is triggered by solvent polarity.[5c] In particular, the formation of flexible coil-like cylindrical aggregates in aqueous solution is attributed to the aggregation of branched hydrophobic chains into amorphous cylindrical cores. Thus, the addition of aromatic guest molecules into the hydrophobic core should force the Y-shaped aromatic segments, which are radially distributed, to be arranged in a more dense, parallel packing and so bind the guest efficiently. This rearrangement could result in a structural change of the 1D assembly into larger aggregates to maximize the parallel packing of the aromatic segments (Figure 1). The guest molecules could then be considered as

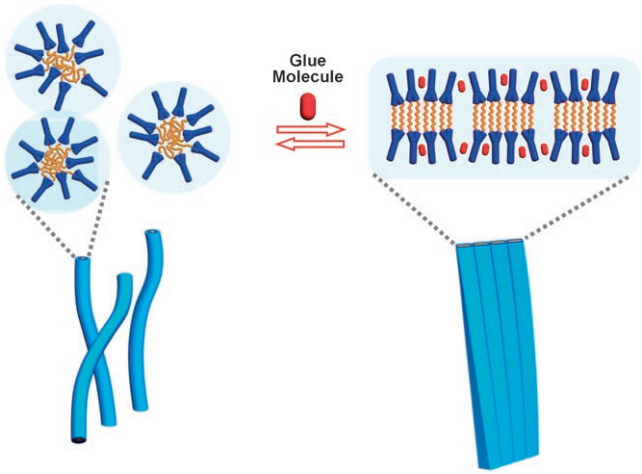

Figure 1. Schematic representation of the transformation of single nanofibers to flat ribbons driven by "molecular glue".

"molecular glue" because they stick individual aromatic segments to one another, which subsequently leads to the formation of larger aggregates. To substantiate this initial concept, we have investigated the self-assembly of wedge-coil block molecules based on a Y-shaped aromatic segment containing a linear poly(ethylene oxide) (PEO) group at the tail and branched alkyl chains at the head.

We present herein the formation of cylindrical fibers by the self-assembly of wedge-shaped amphiphiles in aqueous solution and lateral association of the fibers into flat ribbons triggered by the addition of aromatic guest molecules (Figure 1). The synthesis of the wedge-coil molecules (**1**–**3**) was achieved in a stepwise fashion according to procedures described previously.[6] All the analytical data for **1**–**3** are in full agreement with their chemical structures.

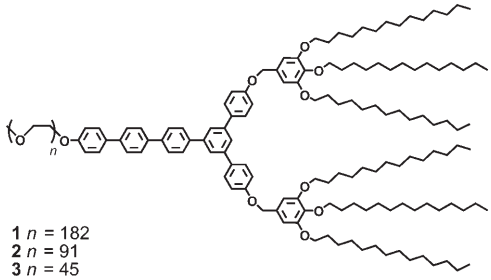

1 *n* = 182
2 *n* = 91
3 *n* = 45

[*] E. Lee, J.-K. Kim, Prof. M. Lee
Center for Supramolecular Nanoassembly and
Department of Chemistry
Yonsei University
Shinchon 134, Seoul 120-749 (Korea)
Fax: (+82) 2-393-6096
E-mail: mslee@yonsei.ac.kr
Homepage: http://csna.yonsei.ac.kr

[**] This work was supported by the National Creative Research Initiative Program of the Korean Ministry of Science and Technology. E.L. and J.-K.K acknowledge fellowships from the BK21 program of the Ministry of Education and Human Resources Development.

Supporting information for this article is available on the WWW under http://dx.doi.org/10.1002/anie.200801496.

The aggregation behavior of **1**, **2**, and **3** was studied in aqueous solution by fluorescence spectroscopy. The emission maxima of the molecules in aqueous solution (2.5×10^{-3} M) were red-shifted with respect to those recorded in chloroform, and their fluorescence is quenched, which indicates aggregation of the aromatic segments (Figure S2 in the Supporting Information).[7] Dynamic light scattering (DLS) measurements were made on aqueous solutions (0.01 wt %) of the amphiphiles to investigate the aggregation behavior further. The CONTIN analysis of the autocorrelation function of **1** shows a narrow size distribution, indicating well-equilibrated structures. Compunds **2** and **3** exhibit trimodal distributions corresponding to unimers, micelles, and larger aggregates (Figure S3 in the Supporting Information).[8] The micellar aggregates, which dominate in solution, have an average hydrodynamic radius of approximately 101 nm and 67 nm for **2** and **3**, respectively.

Transmission electron microscopy (TEM) experiments were performed on aqueous solutions of **1**–**3** to further confirm the structure of the aggregates. Cryogenic-TEM (cryo-TEM) investigations were also carried out in aqueous solution to provide direct visualization of the aggregate structures formed in water.[9] Compound **1**, which is based on a long PEO chain, self-assembles into a spherical aggregate. When a sample was cast from an aqueous solution (0.01 wt %) and then negatively stained with uranyl acetate, the image showed spherical objects with a uniform diameter of 28 nm (Figure S4 in the Supporting Information). The cryo-TEM image revealed the presence of spherical micelles with an average diameter of 10 nm against the vitrified solution background (Figure 2a). The hydrophobic cores appeared to

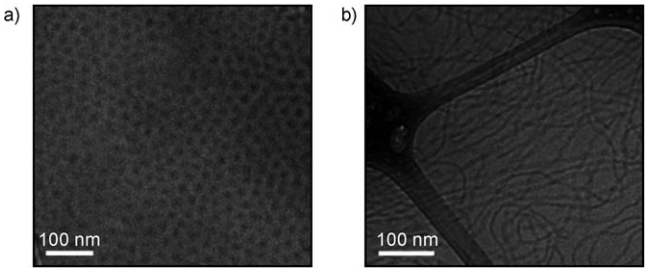

Figure 2. Cryo-TEM images showing the a) spherical morphology of **1** and b) long cylindrical morphology of **3** in aqueous solution (0.01 wt %).

be dark, whereas the solvated PEO coils were not directly visible.[10] The diameter of 10 nm is in reasonable agreement with twice the length of the hydrophobic segment, including the aromatic segments and alkyl chains (ca. 5.4 nm by CPK modeling studies), thus confirming the bilayer packing. A noteworthy feature of this image is the regular hexagonal packing of spheres with a mean separation of about 30 nm. This order seems to be induced by the sample preparation process, and consistent with previous results.[11]

We expected that stronger hydrophobic and π–π stacking interactions between the aromatic segments and a reduction of the interfacial curvature of the nanostructures on decreasing the length of the PEO chain would result in the formation of larger aggregates.[3b,12] TEM images of **2** (with a shorter PEO chain) cast onto a TEM grid from a 0.01 wt % solution showed the coexistence of spherical and short cylindrical micelles with a uniform diameter of 23 nm (Figure S4 in the Supporting Information).[13] As expected, a further decrease in the length of the PEO coils drives the system to form long nanofibers. The TEM image of **3** (from a 0.01 wt % solution) shows cylindrical objects with a uniform diameter of 19 nm and lengths of at least several micrometers (see Figure S4 in the Supporting Information). The formation of the long fibers in aqueous solution was further confirmed by cryo-TEM. The image clearly revealed dark, long, entangled cylindrical micelles with a uniform diameter of approximately 10 nm against the vitrified solution background (Figure 2b). It should be noted that the observed diameter is smaller than the result obtained from a cast film. This is because hydrated PEO chains do not provide sufficient contrast for direct observation.[10] Decreasing the length of the hydrophilic PEO coils therefore reduces the interfacial curvature and can thus give rise to the transformation of spherical micelles to extended cylindrical aggregates.

Interestingly, the diameter (ca. 10 nm) of the hydrophobic core in the cylindrical micelles of **3** is very close to that of the spherical core of **1**, which suggests that the aromatic segments in the cylindrical cores are stacked in a more radial arrangement. This finding led us to investigate if the addition of aromatic guests into the micellar solution would drive the loose radial packing of the aromatic segments to a closer parallel packing through a "glue action" of the guest molecules, thereby transforming 1D cylindrical micelles into larger aggregates (Figure 1). Indeed, the elementary fibers of **3** were observed to associate laterally into flat ribbons upon addition of Nile Red dye. DLS experiments showed that both relaxation time and average hydrodynamic radii (R_H) of the solution of **3** increased when the amount of Nile Red added was increased to 20 mol %. These observations reflect an increase in the size of the aggregate upon guest binding (Figure 3a,b).

To corroborate the structural change upon addition of the guest molecule, TEM was carried out on a solution of **3** containing Nile Red. The micrograph of the unstained sample revealed ribbonlike aggregates with lengths of up to several micrometers (Figure 3c). Close examination of the samples negatively stained with uranyl acetate revealed that the flat ribbons consist of laterally stacked elementary fibers (Figure 3d). The density profile perpendicular to the long axis of the ribbon showed an interfiber distance of about 18 nm, which is consistent with the diameter of the single fibers. This finding indicates that the cylindrical fibers are laterally associated into flat ribbons on addition of the aromatic guest. The formation of ribbons was further confirmed by cryo-TEM and scanning electron microscopy, which also revealed the presence of ribbons with widths ranging from several tens to several hundreds of nanometers (Figures S6 and S7 in the Supporting Information). This trend is in good agreement with the results obtained by DLS measurements. Full recovery of the original fibers was observed by DLS and cryo-TEM (Figure S8 in the Supporting Information) upon removal of the guest molecule by extraction with *n*-hexane.

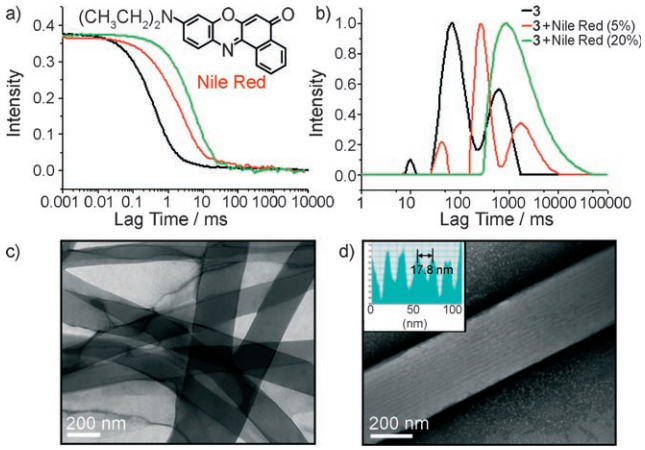

Figure 3. a) Autocorrelation functions and b) size distribution graphs at a scattering angle 90° from CONTIN analysis of the autocorrelation function from the laser light scattering of an aqueous solution of **3** (0.01 wt%) and a solution (0.01 wt%) of **3** and Nile Red (5–20 mol% relative to **3**). c) TEM image (unstained) of **3** containing Nile Red (10 mol%). d) TEM image and density profile of **3** containing Nile Red (10 mol%), with negative staining showing that the fibers are associated into flat ribbons.

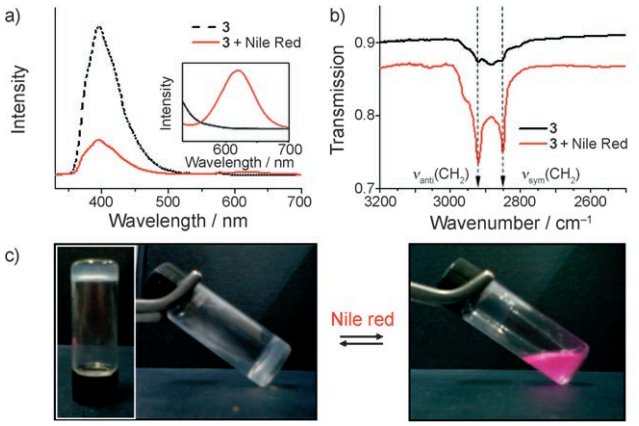

Figure 4. a) Emission spectra (λ_{ex} = 298 nm) of a solution of **3** (2.5×10^{-3} M) and a solution of **3** (2.5×10^{-3} M) and Nile Red (10 mol% relative to **3**). b) FTIR spectra (2500–3200 cm^{-1}) of an aqueous solution of **3** (0.1 wt%) and a solution of **3** and Nile Red (0.1 wt%). c) Photographs of the reversible sol–gel phase transition upon addition of Nile Red (2 wt%).

This result demonstrates that the single fibers of **3** reversibly associate into flat ribbons on addition of a hydrophobic aromatic guest molecule.

The reversible association can be explained by considering the intercalation of Nile Red between the aromatic segments of the wedge-coil block molecule (Figure 1). This process drives the Y-shaped aromatic segments from a radial arrangement to one in which they are mutually parallel to bind the guests efficiently through π–π stacking interactions. Subsequently, the cylindrical fibers associate laterally into larger aggregates to increase the extent of the parallel packing of the aromatic segments; a simultaneous decrease in the unfavorable contact between the hydrophobic side faces and water molecules is also observed. The intercalation of Nile Red within the aromatic segments was confirmed by fluorescence spectroscopy. When a solution of **3** containing Nile Red was excited at 298 nm, where most of the radiation is absorbed by **3**, the fluorescence intensity of **3** was suppressed while a strong emission at 620 nm, corresponding to energy transfer from **3** to Nile Red, was observed. This result clearly indicates that strong π–π stacking interactions exist between the Y-shaped aromatic segments and the Nile Red molecules (Figure 4a).[14–16]

The induced order of the hydrophobic segments by the Nile Red molecules was also shown in the FTIR spectra (Figure 4b). The IR bands at 2918 cm^{-1} (ν_{anti}) and 2850 cm^{-1} (ν_{sym}), which contribute to modes corresponding to CH_2 stretching vibrations, are sensitive to the crystalline packing of alkyl chains.[4a,17] The films of pure **3** cast from an aqueous solution (0.1 wt%) showed only small, broad bands in this region of the spectrum, thus indicating that the hydrophobic cores containing the alkyl chains are disordered. In great contrast, the films of **3** containing Nile Red showed strong, sharp IR bands, indicative of a high crystallinity of the alkyl chains. The disordered hydrophobic segments are therefore rearranged into a much more ordered structure upon addition of aromatic guest molecules.

The bulky dendritic architecture of the hydrophobic cylindrical core can be considered to frustrate the crystallization process, which prevents the dense packing of the dendritic segments. Upon addition of aromatic guests to the cylindrical fibers, however, attractive π–π stacking interactions dominate and enforce alignment of the loosely packed aromatic segments in a parallel arrangement, thus allowing the aromatic segments to bind guest molecules efficiently through maximized π–π interactions. This rearrangement of the aromatic segments within the core of the cylinders results in the hydrophobic exteriors of the cylindrical micelles being exposed to water molecules. To reduce the energetic penalty associated with this unfavorable contact, the elementary fibers associate laterally to form 2D ribbons (Figure 1). Consequently, the cylindrical fibers recognize aromatic guest molecules, which act as "molecular glue" by adhering the single fibers to each other to form ribbonlike layer aggregates.

An inherent property of elongated cylindrical micelles is the possibility to form macroscopic gels.[5a,b,18] To confirm the gelation behavior of the cylindrical fibers, **3** was dissolved in an aqueous solution containing 10% ethanol, which formed gels at concentrations above 2 wt%. Upon addition of Nile Red, which forces the entangled cylindrical micelles to transform into a flat 2D structure, the gels rapidly become fluid solutions (Figure 4c). These results demonstrate that the "molecular glue" can be used to trigger a reversible sol–gel phase transition.

In summary, the results described herein demonstrate that, as the length of the hydrophilic PEO chain in the rigid wedge/flexible coil diblock molecules decreases, the self-assembled structures change from spherical micelles to short fibers and finally to long fibers. Notably, the cylindrical nanofibers were further observed to reversibly aggregate to form flat ribbons on addition of aromatic guest molecules.

Therefore, a key feature of these cylindrical nanofibers, compared to other self-assembled 1D systems,[1c,5,14,18a,19] is their ability to adhere laterally to each other to form larger 2D aggregates, a process driven by small molecules that function as a dynamic "molecular glue". In addition, this dynamic fibrillar association leads to a macroscopic switching of the bulk solution from a gel to a fluid solution. These results represent a significant example of dynamic structural variation triggered by external stimuli in a self-assembling system, thus providing a useful strategy to create intelligent nanoscale materials with predefined functions.

Received: March 30, 2008
Published online: July 10, 2008

Keywords: aggregation · intercalation · nanostructures · self-assembly · supramolecular chemistry

[1] a) J.-M. Lehn, *Proc. Natl. Acad. Sci. USA* **2002**, *99*, 4763 – 4768; b) S. Förster, T. Plantenberg, *Angew. Chem.* **2002**, *114*, 712 – 739; *Angew. Chem. Int. Ed.* **2002**, *41*, 688 – 714; c) F. J. M. Hoeben, P. Jonkheijm, E. W. Meijer, A. P. H. J. Schenning, *Chem. Rev.* **2005**, *105*, 1491 – 1546; d) J. J. L. M. Cornelissen, A. E. Rowan, R. J. M. Nolte, N. A. J. M. Sommerdijk, *Chem. Rev.* **2001**, *101*, 4039 – 4070.

[2] M. Lee, B.-K. Cho, W.-C. Zin, *Chem. Rev.* **2001**, *101*, 3869 – 3892.

[3] a) E. R. Zubarev, M. U. Pralle, E. D. Sone, S. I. Stupp, *J. Am. Chem. Soc.* **2001**, *123*, 4105 – 4106; b) J.-K. Kim, E. Lee, Z. Huang, M. Lee, *J. Am. Chem. Soc.* **2006**, *128*, 14022 – 14023; c) W.-Y. Yang, E. Lee, M. Lee, *J. Am. Chem. Soc.* **2006**, *128*, 3484 – 3485; d) D. M. Vriezema, J. Hoogboom, K. Velonia, K. Takazawa, P. C. M. Christianen, J. C. Maan, A. E. Rowan, R. J. M. Nolte, *Angew. Chem.* **2003**, *115*, 796 – 800; *Angew. Chem. Int. Ed.* **2003**, *42*, 772 – 776.

[4] a) J. P. Hill, W. Jin, A. Kosaka, T. Fukushima, H. Ichihara, T. Shimomura, K. Ito, T. Hashizume, N. Ishii, T. Aida, *Science* **2004**, *304*, 1481 – 1483; b) A. Aggeli, I. A. Nyrkova, M. Bell, R. Harding, L. Carrick, T. C. B. McLeish, A. N. Semenov, N. Boden, *Proc. Natl. Acad. Sci. USA* **2001**, *98*, 11857 – 11862.

[5] a) H.-J. Kim, J.-H. Lee, M. Lee, *Angew. Chem.* **2005**, *117*, 5960 – 5964; *Angew. Chem. Int. Ed.* **2005**, *44*, 5810 – 5814; b) K.-S. Moon, H.-J. Kim, E. Lee, M. Lee, *Angew. Chem.* **2007**, *119*, 6931 – 6934; *Angew. Chem. Int. Ed.* **2007**, *46*, 6807 – 6810; c) J.-K. Kim, E. Lee, M. Lee, *Angew. Chem.* **2006**, *118*, 7353 – 7356; *Angew. Chem. Int. Ed.* **2006**, *45*, 7195 – 7198.

[6] a) J. Bae, J.-K. Kim, N.-K. Oh, M. Lee, *Macromolecules* **2005**, *38*, 4226 – 4230; b) J.-K. Kim, M.-K. Hong, J.-H. Ahn, M. Lee, *Angew. Chem.* **2005**, *117*, 332 – 336; *Angew. Chem. Int. Ed.* **2005**, *44*, 328 – 332; c) S. Peleshanko, J. Jeong, V. V. Shevchenko, K. L. Genson, Y. Pikus, M. Ornatska, S. Petrash, V. V. Tsukruk, *Macromolecules* **2004**, *37*, 7497 – 7506.

[7] a) B. W. Messmore, J. F. Hulvat, E. D. Sone, S. I. Stupp, *J. Am. Chem. Soc.* **2004**, *126*, 14452 – 14458; b) R. Varghese, S. J. George, A. Ajayaghosh, *Chem. Commun.* **2005**, 593 – 595.

[8] a) A. Kelarakis, V. Castelletto, M. J. Krysmann, V. Havredaki, K. Viras, I. W. Hamley, *Langmuir* **2008**, *24*, 3767 – 3772.; b) K. E. Steege, J. Wang, K. E. Uhrich, E. W. Castner, Jr., *Macromolecules* **2007**, *40*, 3739 – 3748.

[9] a) N. Dan, K. Shimoni, V. Pata, D. Danino, *Langmuir* **2006**, *22*, 9860 – 9865; b) G. Battaglia, A. J. Ryan, *J. Am. Chem. Soc.* **2005**, *127*, 8757 – 8764.

[10] a) Z. Li, E. Kesselman, Y. Talmon, M. A. Hillmyer, T. P. Lodge, *Science* **2004**, *306*, 98 – 101; b) Y. Zheng, Y.-Y. Won, F. S. Bates, H. T. Davis, L. E. Scriven, Y. Talmon, *J. Phys. Chem. B* **1999**, *103*, 10331 – 10334.

[11] Y. He, Z. Li, P. Simone, T. Lodge, *J. Am. Chem. Soc.* **2006**, *128*, 2745 – 2750.

[12] a) Y.-b. Lim, E. Lee, M. Lee, *Angew. Chem.* **2007**, *119*, 9169 – 9172; *Angew. Chem. Int. Ed.* **2007**, *46*, 9011 – 9014; b) E. Lee, Y.-H. Jeong, J.-K. Kim, M. Lee, *Macromolecules* **2007**, *40*, 8355 – 8360.

[13] To directly substantiate the formation of micelles of both shapes, cryo-TEM experiments were performed on a solution of **2** (0.01 wt %, see the Supporting Information).

[14] a) J.-H. Ryu, E. Lee, Y.-b. Lim, M. Lee, *J. Am. Chem. Soc.* **2007**, *129*, 4808 – 4814; b) J.-H. Ryu, H.-J. Kim, Z. Huang, E. Lee, M. Lee, *Angew. Chem.* **2006**, *118*, 5430 – 5433; *Angew. Chem. Int. Ed.* **2006**, *45*, 5304 – 5307.

[15] a) J. Jiang, X. Tong, Y. Zhao, *J. Am. Chem. Soc.* **2005**, *127*, 8290 – 8291; b) J.-H. Ryu, M. Lee, *J. Am. Chem. Soc.* **2005**, *127*, 14170 – 14171.

[16] Evidence for the entrapment of the aromatic substrate by the aromatic segment was further confirmed using pyrene (see the Supporting Information).

[17] G. John, M. Masuda, Y. Okada, K. Yase, T. Shimizu, *Adv. Mater.* **2001**, *13*, 715 – 718.

[18] a) A. Ajayaghosh, V. K. Praveen, *Acc. Chem. Res.* **2007**, *40*, 644 – 656; b) T. Kitahara, M. Shirakawa, S.-i. Kawano, U. Beginn, N. Fujita, S. Shinkai, *J. Am. Chem. Soc.* **2005**, *127*, 14980 – 14981.

[19] A. Aggeli, M. Bell, L. M. Carrick, C. W. G. Fishwick, R. Harding, P. J. Mawer, S. E. Radford, A. E. Strong, N. Boden, *J. Am. Chem. Soc.* **2003**, *125*, 9619 – 9628.

